

Extended Convex Hull-Based Distributed Operation of Integrated Electric-Gas Systems

Rong-Peng Liu, *Student Member, IEEE*, Wei Sun, *Member, IEEE*, Dali Zhou,
and Yunhe Hou, *Senior Member, IEEE*

Abstract—Distributed operation of integrated electricity and gas systems (IEGS) receives much attention since it respects data security and privacy between different agencies. This paper proposes an extended convex hull (ECH) based method to address the distributed optimal energy flow (OEF) problem in the IEGS. First, a multi-block IEGS model is obtained by dividing it into N blocks according to physical and regional differences. This multi-block model is then convexified by replacing the nonconvex gas transmission equation with its ECH-based constraints. The Jacobi-Proximal alternating direction method of multipliers (J-ADMM) algorithm is adopted to solve the convexified model and minimize its operation cost. Finally, the feasibility of the optimal solution for the convexified problem is checked, and a sufficient condition is developed. The optimal solution for the original nonconvex problem is recovered from that for the convexified problem if the sufficient condition is satisfied. Test results reveal that this method is tractable and effective in obtaining the feasible optimal solution for radial gas networks.

Index Terms—Alternating direction method of multipliers, convex relaxation, distributed optimization, integrated electricity and gas systems, optimal energy flow, quadratic programming.

NOMENCLATURE

A. Sets

$\mathcal{D}_p^r/\mathcal{D}_g^{r'}$	Set of power/gas loads in block r/r' .
$\mathcal{G}_p^r/\mathcal{G}_g^r/\mathcal{G}_v^r$	Set of coal-fired/gas-fired/virtual gas-fired generators in block $r/r'/r''$.
$\mathcal{L}_p^r/\mathcal{L}_g^{r'}/\mathcal{C}_g^r$	Set of power transmission lines/gas passive pipelines/gas compressors (gas active pipelines) in block $r/r'/r''$.
$\mathcal{N}_p^r/\mathcal{N}_v^r/\mathcal{N}_g^r$	Set of power/virtual power/gas nodes in block $r/r'/r''$.
\mathcal{W}^r	Set of gas wells in block r' .

B. Constants

$C_p(\cdot)$	Cost function of coal-fired generator.
C_w	Cost of natural gas.
d	Penalty parameter.
G_g^{\min}/G_g^{\max}	Output limits of gas-fired generator.
G_i^{\min}/G_i^{\max}	Pressure square limits of gas node.

This work was supported in part by Theme-based Research Scheme (TRS) under T23-701/14-N and in part by National Natural Science Foundation of China under Grant 51677160.

R. Liu and Y. Hou are with the Department of Electrical and Electronic Engineering, the University of Hong Kong, Pokfulam Road, Hong Kong. Y. Hou is also with the University of Hong Kong Shenzhen Institute of Research and Innovation, Shenzhen 518057, China (e-mail: rpliu@eee.hku.hk; yhou@eee.hku.hk).

W. Sun is with the Department of Electrical and Computer Engineering, University of Central Florida, Orlando, FL 32186 USA (e-mail: sun@ucf.edu).

D. Zhou is with the China National Heavy Duty Truck Group Co., Ltd., Jinan 250000, China (e-mail: zhoudali1992@sina.com).

G_l^{\min}/G_l^{\max}	Transmission limits of gas passive pipeline.
G_w^{\min}/G_w^{\max}	Output limits of gas well.
P_d/G_d	Nodal loads of power/gas network.
P_g^{\min}/P_g^{\max}	Output limits of coal-fired generator.
P_l/G_c	Transmission limit of power transmission line/gas compressor.
W_l	Weymouth equation constant.
x_l	Reactance of power transmission line.
a_l	Gas compressor constant.
γ	Damping parameter.
$\theta_i^{\min}/\theta_i^{\max}$	Phase angle limits of power node.
χ_g	Electricity-gas conversion ratio.

C. Variables

g_w	Output of gas well.
g_g^j	Output of virtual gas-fired generator.
p_g/g_g	Output of coal-fired/gas-fired generator.
$p_l/g_l/g_c$	Power/gas/gas flow through power transmission line/gas passive pipeline/gas compressor.
θ_i/π_i	Phase angle/pressure square of power/gas node.
θ_i^j	Phase angle of virtual power node.
λ	Lagrangian multiplier.

I. INTRODUCTION

Traditional power generation relies heavily on coal and causes severe environmental related problems. Seeking alternatives is imperative. Natural gas is a feasible solution due to its eco-friendly and low-cost properties. Thanks to the shale gas revolution and tax credit [1], natural gas has been one of the largest sources of energy for electricity generation, especially in the U.S. and the U.K. [2], [3]. Hereinafter, the word “gas” refers to both the underground natural gas and the natural gas extracted from the shale rock.

Bulk integrated electricity and gas system (IEGS) is constructed to facilitate the gas-fired generation, and the optimal energy flow (OEF) problem in the IEGS has attracted many researchers’ attention. However, the IEGS also brings new challenges which are caused by complex coupling relations, e.g., synergistic expansion, synchronous dispatch, and security problems. Some research work is conducted to address these challenges [4]–[9]. Specifically, reference [4] proposes a co-expansion planning model considering market-related factors. Reference [5] applies an expansion model to the integrated electric-gas-heat system. A practical OEF model is proposed in [6], in which only a limited number of components can be adjusted. Reference [7] proposes an optimal operation strategy for the IEGS with power-to-gas conversion facilities. In [8], security constraints are incorporated into the IEGS to ensure its feasibility under pre-defined security conditions. Reference [9]

adopts a two-stage robust optimization model to enhance the resilience of the integrated electric-gas distribution systems against natural disasters.

Previous work mainly focuses on the centralized operation. In practice, power and gas networks usually belong to different companies. Even a connected power network may be divided into several blocks by region, with each block managed by an agency. From the perspective of security and privacy, it is risky and unrealistic to share all the information between different companies and agencies. *Distributed operation* is a promising solution, which leads to distributed optimization problems [10], [11]. The alternating direction method of multipliers (ADMM) algorithm [12] is widely employed to solve these problems due to the promising performance [13]-[16]. However, challenges still exist when addressing distributed OEF problems for the IEGS by the ADMM algorithm: i) systematic block partitioning method; ii) convergence guarantee of ADMM algorithms when the number of partitioned blocks is larger than two; iii) nonconvex constraints in the gas block.

Recent studies provide some methods to address these challenges. According to the physical difference, reference [13] divides the IEGS into two blocks, i.e., power and gas blocks. The second-order cone (SOC) relaxation method [17] is adopted to relax nonconvex gas transmission equations, and the relaxed model is solved by the standard ADMM algorithm. In [14], during each iteration of the standard (two-block) ADMM algorithm, the local optimal solution for the nonconvex gas block is obtained by the convex-concave procedure (CCP) [18]. Reference [15] adopts the same two-block partitioning method, and nonconvex gas constraints are linearized by the piecewise linearization (PWL) method [19]. The OEF problem is solved by the tailored ADMM algorithm [20]. Differently, reference [16] divides the IEGS into N ($N \geq 2$) blocks by region. The sequential cone programming method is leveraged to handle the nonconvex gas block, and the iterative ADMM is proposed to solve the IEGS model. In this paper, we try to address the aforementioned challenges i)-iii) in the following ways:

- i) *Block partitioning method*: Physical and regional partitioning standards are employed separately in previous work [13]-[16]. In practice, they could coexist. The construction of the multi-block IEGS model considering both standards is worth a try.
- ii) *Distributed optimization*: According to [21], the direct extension of the two-block ADMM algorithm to multi-block distributed optimization problems does not necessarily converge. The Jacobi-Proximal ADMM (J-ADMM) algorithm [22], which is provably convergent when addressing multi-block distributed optimization problems, applies to solve the distributed OEF problem for the multi-block IEGS.
- iii) *Convexified model*: The basic convergence condition of the J-ADMM algorithm is that all blocks are convex [22]. However, the gas block model is nonconvex due to the gas transmission equation. Model convexification is a plausible method and has received success in power systems [23]. A specific convex relaxation method for the gas block is worth studying. Besides, the optimal solution for the convexified problem may not be feasible for the original problem. The solution feasibility needs to be carefully checked.

Overall, this paper aims to address the distributed OEF problem for the IEGS. Contributions are as follows:

1) *Distributed operation*. A block partitioning method, which considers both physical and regional differences in the IEGS, is proposed to decouple the IEGS into N ($N \geq 2$) blocks. To the best of the authors' knowledge, this is the first work to decouple the IEGS by leveraging both physical and regional differences. Then, coupling relations between decoupled blocks are utilized to formulate the multi-block IEGS model. The J-ADMM algorithm is adopted to address the distributed OEF problem for the multi-block model. This algorithm allows parallel computing, which notably improves its computational efficiency.

2) *Extended convex hull (ECH) based relaxation method*. A convexified IEGS model is proposed by replacing nonconvex gas transmission equations with ECH-based constraints. Compared with [13], [15], [16], the proposed method does not introduce binary variables to the distributed OEF problem, which ensures its convergence; compared with [14], [24], the bi-directional property of gas passive pipelines is respected, which increases the gas transmission flexibility. In addition, the feasibility of the solution is checked, and a sufficient condition is developed. The optimal solution for the original nonconvex problem is recovered from that for the convexified problem if the sufficient condition is satisfied. Test results reveal that this method is effective in obtaining the feasible optimal solution for radial gas networks.

The remainder of this paper is constructed as follows. Section II introduces the decoupling method and the mathematical formulation of the multi-block IEGS. The ECH, the J-ADMM algorithm, and the solution feasibility check and recovery method are discussed in Section III. Simulation results are presented in Section IV. Section V concludes this paper.

II. PROBLEM FORMULATION

In this section, a block partitioning method is proposed to construct the multi-block IEGS model, and the mathematical formulation of power and gas blocks are presented. Before that, we make the following assumptions and simplifications:

1) The single-period OEF problem is studied. It can be extended to multi-period problems, regardless of whether unit commitment (UC) variables, i.e., binary variables, are included [15], [16]. Note that the optimal solution for the multi-block UC problem solved by the ADMM algorithm may not be globally optimal.

2) The IEGS is firstly divided into one power network and one gas network. Then, the power network is further divided into multiple blocks. For the sake of simplicity, the gas network is no longer partitioned by assuming that it belongs to one gas company. The proposed partitioning method for the power network can be directly extended to the gas network.

3) The direct current (DC) power flow equation is employed to characterize the relation between the power flow and the phase angle variables. This equation is widely applied to power transmission networks [8], [15], [16].

4) The uncertainty of power and gas loads is ignored, as this paper mainly focuses on the distributed operation.

A. Block Partitioning method

The power and gas networks usually belong to different companies. Distributed operation is a promising approach to guard data security and privacy. Based on physical differences, the power network is decoupled from the gas network. Gas-fired generators are coupling components that connect these two networks, and the coupling relation is shown in the upper portion of Fig. 1. The dotted line denotes the gas supplied to the gas-fired generator g from the gas node j . Gas-fired generators are considered to belong to power blocks. As is shown in the lower portion of Fig. 1, a virtual gas-fired generator g' is added to the gas node j to help in decoupling the power block from the gas block.

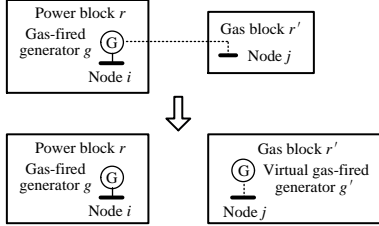


Fig. 1. Decoupling method between power and gas blocks.

The decoupled power network is further partitioned into several blocks by region, as power blocks in different regions usually belong to different agencies. Power transmission lines that connect different blocks are coupling components, and the coupling relation is shown in the upper portion of Fig. 2. Power blocks r_1 and r_2 are connected by a power transmission line l (solid line). As is shown in the lower portion of Fig. 2, virtual power nodes j' and i' are added to power blocks r_1 and r_2 , respectively. The original power transmission line l is separated into two lines to connect the actual and the virtual nodes in these two blocks, respectively. By repeating this partitioning method, the power network is decoupled into multiple power blocks.

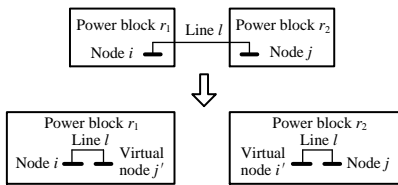


Fig. 2. Decoupling method between two power blocks.

B. Power Block Model

The mathematical model of each decoupled power block r ($r = 1, \dots, N-1$) is demonstrated as follows:

$$\min_{\mathbf{a}_p \in \Omega_p^r} \sum_{g \in \mathcal{G}_p^r} C_p(p_g) \quad (1)$$

$$P_g^{\min} \leq P_g \leq P_g^{\max} \quad g \in \mathcal{G}_p^r \quad (2)$$

$$G_g^{\min} \leq g_g \leq G_g^{\max} \quad g \in \mathcal{G}_p^r \quad (3)$$

$$\theta_i^{\min} \leq \theta_i \leq \theta_i^{\max} \quad i \in \mathcal{N}_p^r \quad (4)$$

$$-P_l \leq p_l \leq P_l \quad l \in \mathcal{L}_p^r \quad (5)$$

$$x_l \cdot p_l = \begin{cases} \theta_{i(l)} - \theta_{j(l)} & \text{both power nodes are actual} \\ \theta_{i(l)} - \theta_{j'(l)} & \text{one power node is virtual} \end{cases} \quad l \in \mathcal{L}_p^r \quad (6)$$

$$\sum_{g_p \in \mathcal{G}_p^r} p_{g_p(i)} + \sum_{g_g \in \mathcal{G}_p^r} g_{g_g(i)} + \sum_{l_1 \in \mathcal{L}_p^r} p_{l_1(i)} - \sum_{l_2 \in \mathcal{L}_p^r} p_{l_2(i)} = \sum_{d \in \mathcal{D}_p^r} P_{d(i)}$$

$$i \in \mathcal{N}_p^r. \quad (7)$$

Objective function (1) aims to minimize the generation cost of coal-fired generators, where $C_p(p_g) = c_1 \cdot p_g^2 + c_2 \cdot p_g + c_3$ is quadratic ($c_1 \geq 0$). The generation cost of gas-fired generators is not included. Function (1) is convex (but not necessarily strongly convex).

The feasible region of each power block r , Ω_p^r , consists of (2)-(7). Vector \mathbf{a}_p is composed of the variables in these constraints. Constraints (2) and (3) enforce the output capacity of coal-fired and gas-fired generators, respectively. Constraint (4) indicates that the phase angle cannot exceed its boundary. Constraint (5) states the thermal limit of a power transmission line. Constraint (6) is the DC power flow equation, where $i(l)$ and $j(l)$ denote a pair of actual power nodes connected by line l , while $j(l')$ denotes the virtual power node. Constraint (7) is the power balance equation, where $g_p(i)$, $g_g(i)$, $l_1(i)$, $l_2(i)$, and $d(i)$ denote the traditional generator, gas-fired generator, inflow and outflow of power transmission lines, and power loads connecting to power node i , respectively. The power balance constraint for virtual power nodes is not included.

C. Gas Block Model

The mathematical model of the decoupled gas block r' is presented as follows:

$$\min_{\mathbf{a}_g \in \Omega_g^{r'}} \sum_{w \in \mathcal{W}^{r'}} C_w \cdot g_w \quad (8)$$

$$G_w^{\min} \leq g_w \leq G_w^{\max} \quad w \in \mathcal{W}^{r'} \quad (9)$$

$$0 \leq g_c \leq G_c \quad c \in \mathcal{C}_g^{r'} \quad (10)$$

$$G_i^{\min} \leq \pi_i \leq G_i^{\max} \quad i \in \mathcal{N}_g^{r'} \quad (11)$$

$$(g_l)^2 \cdot \text{sgn}(\pi_{i(l)}, \pi_{j(l)}) = W_l \cdot (\pi_{i(l)} - \pi_{j(l)}) \quad l \in \mathcal{L}_g^{r'} \quad (12)$$

$$\text{sgn}(\pi_{i(l)}, \pi_{j(l)}) = \begin{cases} 1 & \pi_{i(l)} \geq \pi_{j(l)} \\ -1 & \pi_{i(l)} < \pi_{j(l)} \end{cases} \quad l \in \mathcal{L}_g^{r'} \quad (13)$$

$$\pi_{j(c)} \leq \pi_c \cdot \pi_{i(c)} \quad c \in \mathcal{C}_g^{r'} \quad (14)$$

$$\sum_{w \in \mathcal{W}^{r'}} g_{w(i)} + \sum_{l_1 \in \mathcal{L}_g^{r'}} g_{l_1(i)} - \sum_{l_2 \in \mathcal{L}_g^{r'}} g_{l_2(i)} + \sum_{c_1 \in \mathcal{C}_g^{r'}} g_{c_1(i)} - \sum_{c_2 \in \mathcal{C}_g^{r'}} g_{c_2(i)} = \sum_{d \in \mathcal{D}_d^{r'}} G_{d(i)} + \sum_{g_g \in \mathcal{G}_g^{r'}} \chi_g \cdot g_{g_g(i)} \quad i \in \mathcal{N}_g^{r'}. \quad (15)$$

The objective function (8) minimizes the output cost of gas wells and is not strongly convex.

The feasible region for the gas block r' , $\Omega_g^{r'}$, consists of (9)-(15). Vector \mathbf{a}_g is composed of the variables in these constraints. The output capacity of a gas well is bounded by constraint (9). Constraint (10) restricts the gas flow in the gas compressor (gas active pipeline). Constraint (11) states the limits of the pressure square of the gas node. Equation (12) is the Weymouth equation, where $i(l)$ and $j(l)$ denote two gas nodes connected by a gas passive pipeline l . This equation is widely adopted to describe the relationship between the nodal pressure and the gas flow and applies to the high-pressure long-distance gas passive pipeline [25]. Besides, its bi-directional property is depicted by (13). Constraint (14) is a simplified gas compressor (gas active pipeline) model [26], where $j(c)$ and $i(c)$ represent the outflow and inflow nodes connected by the unidirectional gas compressor c . Equation (15) is the gas balance constraint, where

$w(i)$, $l_1(i)$, $l_2(i)$, $c_1(i)$, $c_2(i)$, $d(i)$, and $g'_g(i)$ denote the gas well, inflow and outflow of the gas passive pipeline, inflow and outflow of the gas compressor, gas loads, and virtual gas-fired generator connecting to the gas node i , respectively.

D. Coupling Constraints

Based on the physical and regional differences, the IEGS is divided into several blocks by means of virtual components, i.e., virtual gas-fired generators and virtual power nodes. We utilize the coupling relations between these fully decoupled blocks to formulate the multi-block IEGS model. These coupling relations are presented as follows:

$$\theta_{i(l)} = \theta_{i'(l)} \quad i' \in \bigcup_{r=1}^{N-1} \mathcal{N}_v^r \quad (16)$$

$$g_{g_g(i)} = g_{g'_g(j)} \quad g'_g \in \mathcal{G}_v^{r'} \quad (17)$$

Constraint (16) claims that the phase angle of a virtual power node should be identical to that of the corresponding actual power node. For example, assuming that the virtual power node i' in power block r_2 is a replica of the actual power node i in another power block r_1 (see Fig. 2), the values of phase angles of these two nodes should be the same. Similar equivalent relation between virtual and actual gas-fired generators is presented by (17). The above two coupling constraints ensure the equivalence between the distributed and centralized models.

References [13] and [14] remove coupling constraints directly from the decoupled power and gas blocks. Differently, the proposed method preserves all constraints in each block with the help of virtual components and constructs sparse coupling relations between the decoupled blocks to formulate the multi-block IEGS model. As a result, the complexity of the coupling constraints in the proposed model is greatly reduced.

III. SOLUTION METHOD

In this paper, the J-ADMM algorithm is adopted to solve the distributed OEF problem. Details are in Section III.B. However, its convergence is not guaranteed due to nonconvex Weymouth equations in the gas block. In Section III.A, an ECH-based method is proposed to relax Weymouth equations. Section III.C introduces the solution feasibility check and recovery method.

A. ECH-Based Relaxation Method

The ECH of a set is convex and contains the convex hull of this set. In addition, an ECH should also: i) contain less redundant elements and ii) have a simple analytical form.

Denote the convex hull and the ECH of a set \mathcal{Y} as \mathcal{Y}_{con} and $\mathcal{Y}_{\text{e-con}}$, respectively. According to the above description, $\mathcal{Y}_{\text{e-con}}$ is convex, and the relation $\mathcal{Y}_{\text{con}} \subseteq \mathcal{Y}_{\text{e-con}}$ always holds. The redundant elements refer to the elements which belong to $\mathcal{Y}_{\text{e-con}}$ but do not belong to \mathcal{Y}_{con} . A simple form means that the ECH is depicted by “simple” functions. For example, a linear function is considered simpler than a quadratic function, and a polynomial function is considered simpler than exponential, logarithmic, and trigonometric functions. Thus, the proposed ECH is problem-dependent.

The ECH and the convex hull of the Weymouth equation are shown in Fig. 3. The horizontal axis denotes the difference

between the pressure squares of gas nodes i and j . The vertical axis is the gas flow. The Weymouth equation is depicted by the blue line. In Fig. 3 (a), the region surrounded by red lines is the ECH. It is easy to prove that the red lines and the outermost blue lines in Fig. 3 (b) consist of the boundary of the convex hull.

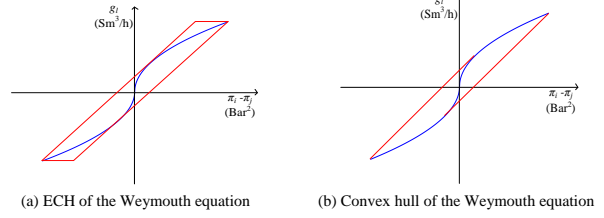


Fig. 3. ECH and convex hull of Weymouth equation.

Compared with the tightest convex relaxation, i.e., the convex hull, the number of redundant elements caused by the proposed ECH is relatively small. However, the ECH is much easier to be characterized analytically. Besides, if the convex hull based constraints are adopted, binary variables will be introduced to the model of the gas block, and the convergence of the ADMM algorithm cannot be guaranteed. In this paper, the Weymouth equation is replaced by ECH-based constraints (see Fig. 3 (a)), and its mathematical formulation is

$$G_l^{\min} \leq g_l \leq G_l^{\max} \quad l \in \mathcal{L}_g^{r'} \quad (18a)$$

$$a_l^L \cdot (\pi_{i(l)} - \pi_{j(l)}) + b_l^L \leq g_l \quad l \in \mathcal{L}_g^{r'} \quad (18b)$$

$$g_l \leq a_l^U \cdot (\pi_{i(l)} - \pi_{j(l)}) + b_l^U \quad l \in \mathcal{L}_g^{r'} \quad (18c)$$

Constraint (18a) sets the upper and lower bounds of the gas flow in a gas passive pipeline. From another perspective, it also states the upper and lower bounds of the ECH. Constraints (18b) and (18c) represent the left and right bounds of the proposed ECH, respectively, where a_l^L , a_l^U , b_l^L , and b_l^U are constants.

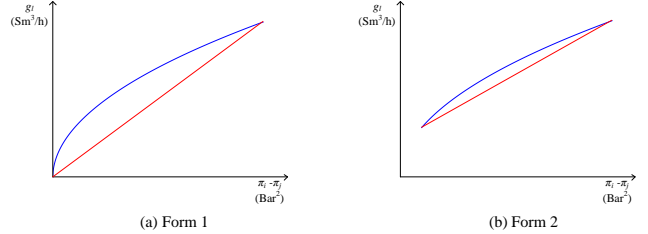


Fig. 4. The other forms of ECHs of Weymouth equations.

Theoretically, the Weymouth equation has the other two forms, besides what has been shown in Fig. 3 (a). These two forms and corresponding ECHs (being the same as their convex hulls) are presented in Fig. 4 (a) and (b), respectively. The blue line denotes the Weymouth equation, and the boundaries of the ECH consist of blue and red lines. Figure 4 (a) shows the scenario when the upper bound of π_j is equal to the lower bound of π_i , and Figure 4 (b) represents another scenario when the upper bound of π_j is smaller than the lower bound of π_i . Figure 4 (a) also applies to the scenario when the gas flow direction is fixed. Both ECHs can be uniformly denoted by

$$a_l^U \cdot (\pi_{i(l)} - \pi_{j(l)}) + b_l^U \leq g_l \quad l \in \mathcal{L}_g^{r''} \quad (19a)$$

$$(g_l)^2 \leq W_l \cdot (\pi_{i(l)} - \pi_{j(l)}) \quad l \in \mathcal{L}_g^{r'}. \quad (19b)$$

Constraints (19a) and (19b) represent the lower and upper boundaries of the proposed ECH, respectively. By replacing the Weymouth equation with ECH-based constraints, the gas block

model, which consists of (8)-(11), (14)-(15), and (18) and/or (19), becomes convex.

B. J-ADMM for Multi-Block IEGS Model

To facilitate understanding, the compact form of the centralized IEGS model, in which the Weymouth equation is replaced by its ECH-based constraints, is displayed as follows:

$$\min_{\mathbf{x}^1, \dots, \mathbf{x}^N} f_1(\mathbf{x}^1) + \dots + f_N(\mathbf{x}^N) \quad (20a)$$

$$\text{s.t. } \mathbf{A}_1 \cdot \mathbf{x}^1 + \dots + \mathbf{A}_N \cdot \mathbf{x}^N = \mathbf{c} \quad (20b)$$

$$\mathbf{x}^i \in \Omega^i, \dots, \mathbf{x}^N \in \Omega^N, \quad (20c)$$

where N ($N \geq 2$) is the number of partitioned blocks. \mathbf{x}^i are the variables which belong to block i ($i = 1, \dots, N$). Ω^i denote convex feasible regions for block i . f_i denote convex objective functions for block i . \mathbf{A}_i refer to constant matrices, and \mathbf{c} is the constant vector. We do not assume f_i are strongly convex.

The procedures for solving the multi-block optimization problem using the J-ADMM algorithm are as follows:

Algorithm 1: J-ADMM algorithm for solving the multi-block distributed OEF problem.

1. Set values of the penalty parameter d , damping parameter γ , matrix \mathbf{P}^r ($r = 1, \dots, N$), stopping criteria ε_1 and ε_2 , maximum number of iterations k_{\max} , and the number of partitioned blocks N . Initialize variables \mathbf{x}_0^r ($r = 1, \dots, N$) and Lagrangian multiplier λ_0 . Set iteration index $k = 0$.
2. Solve the following partitioned blocks in parallel:

$$\mathbf{x}_{k+1}^r = \arg \min_{\mathbf{x}^r \in \Omega_r} f_r(\mathbf{x}^r) + (d/2) \cdot \left\| \mathbf{A}_r \cdot \mathbf{x}^r + \sum_{j \neq r} \mathbf{A}_j \cdot \mathbf{x}_k^j - \mathbf{c} - (\lambda^k / d) \right\|_2^2 + (1/2) \cdot \left\| \mathbf{x}^r - \mathbf{x}_k^r \right\|_{\mathbf{P}^r}^2 \quad r = 1, \dots, N, \quad (21)$$

where $\|\mathbf{x}_m - \mathbf{x}_n\|_{\mathbf{P}}^2 = (\mathbf{x}_m - \mathbf{x}_n)^T \cdot \mathbf{P} \cdot (\mathbf{x}_m - \mathbf{x}_n)$. Obtain the updated values \mathbf{x}_{k+1}^r ($r = 1, \dots, N$). Update Lagrangian multiplier λ_{k+1} according to

$$\lambda_{k+1} = \lambda_k - \gamma \cdot d \cdot \left(\sum_{r=1}^N \mathbf{A}_r \cdot \mathbf{x}_k^r - \mathbf{c} \right). \quad (22)$$

3. Check if both the following stop criteria are satisfied:

$$\left\| \sum_{r=1}^N \mathbf{A}_r \cdot \mathbf{x}_k^r - \mathbf{c} \right\|_2^2 \leq \varepsilon_1 \quad (23)$$

$$\max \left(d \cdot \left\| \mathbf{x}_{k+1}^1 - \mathbf{x}_k^1 \right\|_2^2, \dots, d \cdot \left\| \mathbf{x}_{k+1}^N - \mathbf{x}_k^N \right\|_2^2 \right) \leq \varepsilon_2. \quad (24)$$

If yes, stop and return \mathbf{x}_{k+1}^r ($r = 1, \dots, N$); else if $k = k_{\max}$, stop and return null; else, set $k = k + 1$, and go to Step 2.

According to [22], Algorithm 1 converges to its global optimum if \mathbf{P}^r and γ satisfy the following conditions:

$$\mathbf{P}^r \succ d \cdot \left(\frac{1}{\varepsilon_r} - 1 \right) \cdot \mathbf{A}_r^T \cdot \mathbf{A}_r, \quad r = 1, \dots, N \quad (25)$$

$$\sum_{r=1}^N \varepsilon_r < 2 - \gamma, \quad r = 1, \dots, N. \quad (26)$$

Conditions (25)-(26) are further simplified if $\varepsilon_r < (2 - \gamma)/N$ ($r = 1, \dots, N$), and they are transformed into

$$\mathbf{P}^r \succ d \cdot \left(\frac{N}{2 - \gamma} - 1 \right) \cdot \mathbf{A}_r^T \cdot \mathbf{A}_r, \quad r = 1, \dots, N. \quad (27)$$

Compared with other ADMM algorithms, the J-ADMM algorithm has the following advantages when solving the multi-

block distributed OEF problem:

1) *Convergence.* The global convergence is guaranteed without additional assumptions if the damping parameter γ and matrix \mathbf{P}^r ($r = 1, \dots, N$) are chosen according to (25)-(26) [22]. In contrast, the Gauss-Seidel type ADMM algorithm may not converge when $N \geq 3$ [21], and naïve Jacobi ADMM algorithm may diverge even when $N=2$ [22]. Considering the proposed OEF problem, the number of partitioned blocks may be larger than two. The J-ADMM algorithm ensures its convergence.

2) *Unique solution.* The additional proximal term, $(1/2) \cdot \|\mathbf{x}^r - \mathbf{x}_k^r\|_{\mathbf{P}^r}^2$, ensures that the mathematical formulation of all blocks is strictly convex. Hence, the optimal solution is unique. This is valuable and helpful for system operators to make optimal operation strategies for their blocks, respectively.

3) *Parallel computing.* The J-ADMM algorithm solves all blocks in (21) in parallel. This property is leveraged to speed up the algorithm convergence. In contrast, the Gauss-Seidel type ADMM algorithm can only be implemented in serial.

As aforementioned, the global convergence of Algorithm 1 is guaranteed if conditions (25) and (26) are satisfied. However, it does not mean that the proposed algorithm converges within a certain time. The number of partitioned blocks N and the values of the penalty parameter d and the damping parameter γ also influence computational efficiency to a great extent. In the case study part (Section IV), we will show how these factors impact the algorithm performance.

C. Solution Feasibility Check and Recovery

The optimal solution obtained by solving the convexified problem may not be feasible for the original nonconvex problem, as the feasible region for the original problem is enlarged. Thus, the optimum for (20) may be smaller than that for the original problem. In order to check whether these two optimums are equal without solving the original nonconvex problem, the following theorem is proposed.

Theorem 1: The original and the convexified problems have the same optimum if problem (28) is feasible and its objective value is equal to zero.

$$\min_{\pi, \delta^+, \delta^-} \mathbf{1}^T \cdot \delta^+ + \mathbf{1}^T \cdot \delta^- \quad (28a)$$

$$(g_l^*)^2 \cdot \text{sgn}(g_l^*) = \mathbf{W}_l \cdot (\pi_{i(l)} - \pi_{j(l)}) \quad l \in \mathcal{L}_g^r \quad (28b)$$

$$\text{sgn}(g_l^*) = \begin{cases} 1 & g_l^* \geq 0 \\ -1 & g_l^* < 0 \end{cases} \quad l \in \mathcal{L}_g^r \quad (28c)$$

$$(1 - \delta_i^-) \cdot G_i^{\min} \leq \pi_i \leq (1 + \delta_i^+) \cdot G_i^{\max} \quad i \in \mathcal{N}_g^r \quad (28d)$$

$$\pi_{j(c)} \leq \alpha_c \pi_{i(c)} \quad c \in \mathcal{C}_g^r \quad (28e)$$

$$\delta_i^+, \delta_i^- \geq 0, \quad (28f)$$

where $\delta^+ = (\delta_1^+, \dots, \delta_M^+)^T$ and $\delta^- = (\delta_1^-, \dots, \delta_M^-)^T$ are slack variables.

$M = |\mathcal{N}_g^r|$. g_l^* are the values of the gas flow through gas passive pipeline and are obtained by solving convexified problem (20).

Proof. Assume that π^{**} is a feasible solution for (28). Denote the optimal solution for (20) as \mathbf{x}^* . π^* is the optimal pressure square vector in \mathbf{x}^* . Construct a solution, \mathbf{x}_{opt} , via substituting π^* in \mathbf{x}^* by π^{**} . \mathbf{x}_{opt} is feasible for the original problem, as it satisfies all the constraints, i.e., (2)-(7) and (9)-(17). \mathbf{x}_{opt} and \mathbf{x}^* are equal except the value of π . We notice that changing the

value of π does not influence the objective function values of both original and convexified problems. Thus, their optima are equal. This completes the proof. \blacksquare

This theorem also provides a method to obtain the feasible optimal solution for the original problem.

Corollary 1: Assume that (28) is feasible and its objective value is equal to zero. π^{**} is a feasible solution. Denote the optimal solution for (20) as \mathbf{x}^* . π^* is the optimal pressure square vector. A solution, \mathbf{x}_{opt} , is constructed via replacing π^* in \mathbf{x}^* by π^{**} . \mathbf{x}_{opt} is the optimal solution for the original problem.

Solving the distributed OEF problem, i.e., the original nonconvex problem, is hard. Corollary 1 states if problem (28), a simple linear programming (LP) problem, is feasible and its objective value is equal to zero, the optimum for the original problem is directly obtained, and its feasible optimal solution is recovered from the optimal solution for the convexified problem. If problem (28) is infeasible, a lower bound for the objective value of the original problem is returned. If problem (28) is feasible and its objective value is larger than zero, besides the lower bound, we can also quantify the degree of infeasibility by means of the slack variables δ^+ and δ^- .

IV. CASE STUDY

The proposed methods are tested on two integrated systems, i.e., the 6-node power network with a 7-node gas network and the 118-node power network with a modified 48-node gas network. Detailed system data can be obtained from [27]. Algorithm 1 is coded in MATLAB R2018b. Numerical tests are performed on a PC with an Intel(R) Core(TM) i5-6500 CPU @ 3.20Hz and a 16 GB memory. The solver used to address the quadratic programming (QP) and the MIQP problems is Gurobi 8.1.0. The nonconvex problem (without integer variables) is solved by IPOPT. For the sake of simplicity, condition (27) is adopted in Algorithm 1 to ensure its convergence.

A. Two-Block Case

The 6-node power network with a 7-node gas network is divided into two blocks, i.e., one power block and one gas block. The values of the parameters in Algorithm 1 are shown in Table I, where $\mathbf{M}^r = d \cdot \left(\frac{N}{2-\gamma} - 1\right) \cdot \mathbf{A}_r^T \cdot \mathbf{A}_r$ ($r = 1, \dots, N$).

TABLE I
PARAMETERS SETTING

Parameter	d	γ	\mathbf{P}^r	ε_1	ε_2	k_{\max}
Value	4	1	$1.1 \cdot \mathbf{M}^r$	10^{-4}	10^{-4}	1000

Note that the values of variables included in the coupling constraints should not have a great difference. Otherwise, the variables with large values would dominate the small variables, which could result in convergence difficulties. In this paper, scaling factors are adopted to keep them on the same scale.

B. Solution Feasibility Check and Recovery

To validate the effectiveness of the ECH-based relaxation and solution feasibility check and recovery methods, numerical experiments are conducted under different load profiles. Results are shown in Table II. “Portion” refers to the sum of actual gas well outputs divided by the sum of their maximum output capacities. According to this table, all optimal solutions

for the convexified problem are infeasible (IF) for the original problem, but feasible optimal solutions (for the original problem) are all successfully recovered (Y) from infeasible ones, especially when gas wells nearly reach their output limits (0.99). These results show the effectiveness of the proposed methods. In the following two-block case studies, power and gas loads are fixed to 286 MW and 6,680 Sm³/h, respectively.

TABLE II

RECOVERABILITY TEST UNDER DIFFERENT LOAD PROFILES							
Load profile	Power (MW)	214	243	257	272	286	300
	Gas (Sm ³ /h)	5010	5670	6010	6340	6680	7010
Portion		0.52	0.59	0.67	0.75	0.83	0.91
Feasibility		IF	IF	IF	IF	IF	IF
Recoverability		Y	Y	Y	Y	Y	Y

C. Comparison With Other Methods

The performances of different methods converting the non-convex Weymouth equation to enable the distributed operation are compared, and Table III shows the results. This including the proposed ECH-based relaxation method, the PWL method with eight divided segments, and the SOC relaxation method. Besides, the unidirectional Weymouth equation, shown as

$$(g_l)^2 = \mathbf{W}_l \cdot (\pi_{i(l)} - \pi_{j(l)}) \quad l \in \mathcal{L}_g^{r'}, \quad (29)$$

is employed to obtain a nonconvex model, referred to as the NCV method. Algorithm 1 is adopted to solve the PWL, SOC, NCV, and ECH (ECH-Jacobi) based models. By contrast, the ECH-based model is also solved by the standard ADMM algorithm using Gauss-Seidel iteration method (ECH-Gauss) [12]. “F” and “IF” denote feasible and infeasible, respectively.

TABLE III

COMPARISON BETWEEN DIFFERENT METHODS

Method	Optimality (*10 ⁴ \$)	Number of Iterations	Time (s)	Feasibility
PWL	7.056	31	17.0	F
SOC	7.056	56	218.6	IF
NCV	7.056	30	17.5	F
ECH	Jacobi	7.056	30	F
	Gauss	7.056	11	9.2

In this table, we find out that all the methods are applicable, and the same global optimum is obtained. However, the optimal solution for the SOC based model is infeasible due to the second-order cone relaxation of the Weymouth equation [17]. Besides, the computation time of this model is much longer than that of the others. Similar results of the SOC based model can be found in [14]. The ECH based model solved by Gauss-Seidel iteration method outperforms the others in terms of the running time, although it only allows serial computing.

D. Convergence Performance

The convergence sequences (primal and dual residuals) of the ECH-Jacobi and ECH-Gauss algorithms are presented in Fig. 5 (a) and (b), respectively. The horizontal axis denotes the number of iterations, and the vertical axis is the value of the residual. The same sequence is depicted by two kinds of coordinate systems, i.e., Cartesian coordinate system (left) and semi-logarithmic coordinate system (right), to fully capture the changes. Compared with the standard ADMM algorithm, the J-ADMM algorithm is more difficult to converge. The reason is that the primal and dual residuals (shown in Fig 5 (a)) cannot

decrease simultaneously, although both have a downward trend. Note that the second and the third terms, i.e., $(d/2) \cdot \|\mathbf{A}_r \mathbf{x}^r + \sum_{j \neq r} \mathbf{A}_j \mathbf{x}_k^j - \mathbf{c} - (\lambda^k/d)\|_2^2$ and $(1/2) \cdot \|\mathbf{x}^r - \mathbf{x}_k^j\|_{\mathbf{P}^r}^2$, in (21) exactly denote the primal and dual residuals, respectively. The descent direction of Algorithm 1 is more likely to be dominated by these two terms, alternatively during the iterative process, which leads to the fluctuation and the inconsistently decreasing.

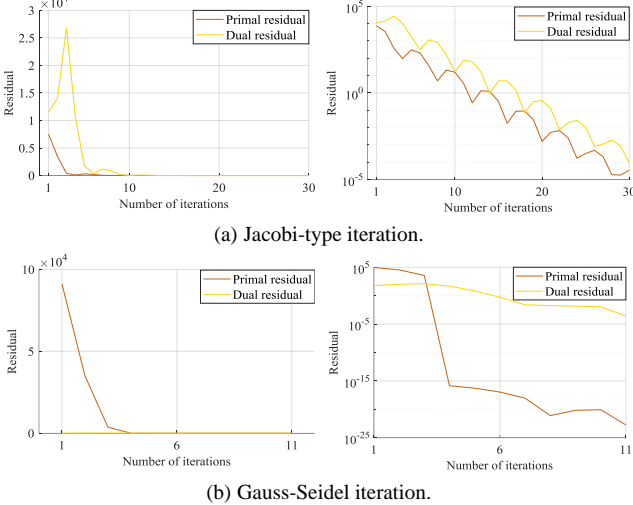


Fig. 5. Convergence sequence comparison.

E. Four-Block Case

In the following subsections, the proposed method is tested on the 118-node power network with a modified 48-node gas network. This IEGS is divided into four blocks, i.e., three power blocks and one gas block. Five compressors are added to gas passive pipe-lines, which leads the gas block to be a “radial” network, as Weymouth equations do not hold for gas active pipelines. Due to the existence of compressors, gas networks are more likely to have the same property as radial networks but remain the meshed structure. Table IV shows the initialized parameters in Algorithm 1. The convergence thresholds of both primal and dual residuals are set to 10^{-2} to balance between the accuracy and the computational cost. The maximum number of iterations is set to 10^4 .

TABLE IV
PARAMETERS SETTING

Parameter	d	γ	\mathbf{P}^r	ε_1	ε_2	k_{\max}	N
Value	1	0.2	$1.1 \cdot \mathbf{M}^r$	10^{-2}	10^{-2}	10^4	4

F. Solution Feasibility Check and Recovery

In this subsection, we continue to investigate the effectiveness of the ECH-based relaxation and solution feasibility check and recovery methods. Test results are shown in Table V. Similar to the results in Section IV.B, feasible optimal solutions for the original problem are recovered from infeasible ones under all load profiles. Compared with the underestimation, the overestimation of the transmission capability of the gas passive pipeline is more likely to result in the failure of the proposed solution recovery method. The overestimation means transmitting a specific amount of gas by a smaller pressure difference (compared with the pressure difference calculated by the Weymouth equation when transmitting the same amount of gas).

It is the redundant elements in the ECH that leads to the overestimated transmission capability. In fact, the overestimation caused by constraints (18) is not very large (see Fig. 3 (a)). This overestimation thoroughly vanishes when constraints (19) are adopted (see Fig. 4). That is why feasible optimal solutions for the original problem can be successfully recovered in both cases.

TABLE V
RECOVERABILITY TEST UNDER DIFFERENT LOAD PROFILES

Load profile	Power (MW)	1250	1500	1750	2125	2375	2500
	Gas (Sm ³ /h)	1350	1620	1890	2295	2565	2700
Portion (%)		51.4	58.4	65.4	75.9	88.6	98.6
Feasibility		IF	IF	IF	IF	IF	IF
Recoverability		Y	Y	Y	Y	Y	Y

G. Gas Transmission Flexibility

We conduct a test to observe gas flow directions under different load profiles, and Table VI shows the results. Actual gas flow directions that agree and disagree with the pre-defined gas flow direction (written as A→B) are denoted by “+” and “-”, respectively. The gas flow direction changes even when the loads have a slight increase (5%). Compared with [14], [24], the proposed ECH-based method respects the bi-directional property of gas flows and thus leads to a more flexible gas block model. In the following four-block case studies, power and gas loads are fixed to 2500 MW and 1580 Sm³/h, respectively.

TABLE VI
GAS TRANSMISSION FLEXIBILITY

Load profile	Power (MW)	1250	1500	1750	2125	2375	2500
	Gas (Sm ³ /h)	1350	1620	1890	2295	2565	2700
Transmission direction	11→12	+	+	+	-	+	+
of gas pipeline	34→35	+	+	+	+	+	-
	37→38	-	-	+	-	+	+

H. Computation Time

As aforementioned, the values of the penalty parameter d and the damping parameter γ greatly impact the computational efficiency. Theoretically, a big penalty term would be added to the objective function if the value of d were too large. As a result, the dual residual would decrease slowly. However, if the value of d were too small, the decline rate of the primal residual would become very slow. Thus, this penalty parameter needs to be chosen within a rational range. In addition, according to (27) and Table IV, the values of matrices \mathbf{P}^r ($r = 1, \dots, N$) are decided by γ and are related to the dual residual term, $(1/2) \cdot \|\mathbf{x}^r - \mathbf{x}_k^j\|_{\mathbf{P}^r}^2$, in the objective function. Thus, the selection of γ also impacts computational efficiency. Simulation results, obtained by solving the ECH-based model using Algorithm 1, are shown in Table VII. Test results show that these two parameters play a key role in deciding the running time of the proposed algorithm.

TABLE VII
INFLUENCE OF PARAMETERS ON COMPUTATION TIME (S)

$\gamma \backslash d$	0.1	0.5	1	2	10
0.01	>3600	2812.0	2751.8	2217.6	>3600
0.1	1597.3	934.2	990.1	1114.6	>3600
0.2	1236.4	618.1	507.3	895.0	2289.0
1.0	1410.4	805.3	1389.3	1407.2	>3600
1.5	959.4	1604.2	1387.1	1849.4	>3600
1.9	>3600	>3600	>3600	>3600	>3600

I. Comparison With Other Methods

Similar to the comparison in Section IV.C, different model converting methods, which enable the distributed operation, are tested. Results are shown in Table VIII. Algorithm 1 is used to solve PWL, SOC, NVC, and ECH based models. Besides, the direct extension of the standard ADMM algorithm is used to solve the proposed multi-block problem (ECH-Gauss). Binary variables are introduced to PWL and SOC based models, which leads to nonconvex mixed-integer programming problems, and both of them fail to converge within ten hours. The NCV-based model does not converge either within ten hours due to nonconvex Weymouth equations. The proposed ECH-based model (leading to a convex QP problem) converges under both algorithms. Algorithm 1, which allows parallel computing, outperforms the ECH-Gauss algorithm on the running time, although the former takes more iterations to converge.

TABLE VIII

COMPARISON BETWEEN DIFFERENT METHODS

Method	Optimality (*10 ⁵ \$)	Number of iterations	Time (s)	Feasibility
PWL	-	-	>3.6*10 ⁴	-
SOC	-	-	>3.6*10 ⁴	-
NCV	-	-	>3.6*10 ⁴	-
ECH	Jacobi	1.340	976	507.3
	Gauss	1.340	789	1541.1

V. CONCLUSION

This paper proposes an ECH-based multi-block model to address the distributed OEF problem in the multi-block IEGS. Specifically, the nonconvex Weymouth equation is replaced by the ECH-based constraints and thus convexified. The J-ADMM algorithm is adopted to solve this convexified problem. After that, the feasibility of the optimal solution for the convexified problem is checked, and a sufficient condition is developed. The optimal solution for the original nonconvex problem is recovered from that for the convexified problem if the sufficient condition is satisfied. Simulation results show that: i) The J-ADMM algorithm is effective and efficient to solve multi-block distributed OEF problems; ii) The penalty parameter d and the damping parameter γ greatly influence the running time of the J-ADMM algorithm; iii) Though only a sufficient condition, it is quite effective to help to obtain a feasible optimal solution for radial gas networks under different load profiles. According to [28], the tested multi-block ADMM outperforms the two-block ADMM on both performance and running time, which is consistent with our conclusion. Future work includes developing a new solution recovery method for meshed gas networks.

REFERENCES

- [1] R. S. Middleton, R. Gupta, J. D. Hyman, and H. S. Viswanathan, "The shale gas revolution: Barriers, sustainability, and emerging opportunities," *Applied Energy*, vol. 199, no.1, pp. 88-95, Aug. 2017.
- [2] U.S. Energy Information Administration. Annual Energy Review, 2018 [Online]. Available: <https://www.eia.gov/totalenergy/data/annual/index.php>
- [3] National statistics. Electricity Generation, Trade and Consumption, 2018. [Online]. Available: <https://www.gov.uk/government/statistics/electricity-section-5-energy-trends>
- [4] J. Qiu, Z. Y. Dong, J. H. Zhao, K. Meng, Y. Zheng and D. J. Hill, "Low carbon oriented expansion planning of integrated gas and power systems," *IEEE Trans. Power Syst.*, vol. 30, no. 2, pp. 1035-1046, March 2015.
- [5] W. Yang, W. Liu, C. Y. Chung and F. Wen, "Coordinated planning strategy for integrated energy systems in a district energy sector," *IEEE Trans. Sustain. Energy*, in press (early access).
- [6] S. Chen, Z. Wei, G. Sun, Y. Sun, H. Zang and Y. Zhu, "Optimal power and gas flow with a limited number of control actions," *IEEE Trans. Smart Grid*, vol. 9, no. 5, pp. 5371-5380, Sept. 2018.
- [7] Y. Li, W. Liu, M. Shahidehpour, F. Wen, K. Wang and Y. Huang, "Optimal operation strategy for integrated natural gas generating unit and power-to-gas conversion facilities," *IEEE Trans. Sustain. Energy*, vol. 9, no. 4, pp. 1870-1879, Oct. 2018.
- [8] C. M. Correa-Posada and P. Sánchez-Martin, "Security-constrained optimal power and natural-gas flow," *IEEE Trans. Power Syst.*, vol. 29, no. 4, pp. 1780-1787, July 2014.
- [9] C. He, C. Dai, L. Wu and T. Liu, "Robust network hardening method for enhancing resilience of integrated electricity and natural gas distribution systems against natural disasters," *IEEE Trans. Power Syst.*, vol. 33, no. 5, pp. 5787-5798, Sept. 2018.
- [10] T. Erseghe, "Distributed Optimal Power Flow Using ADMM," *IEEE Trans. Power Syst.*, vol. 29, no. 5, pp. 2370-2380, Sept. 2014.
- [11] D. Xu, Q. Wu, B. Zhou, C. Li, L. Bai and S. Huang, "Distributed multi-energy operation of coupled electricity, heating and natural gas networks," *IEEE Trans. Sustain. Energy*, in press (early access).
- [12] S. Boyd, N. Parikh, B. Peleato, and J. Eckstein, "Distributed optimization and statistical learning via the alternating direction method of multipliers," *Found. Trends in Mach. Learn.*, vol. 3, no. 1, pp.1-122, 2011.
- [13] Y. Wen, X. Qu, W. Li, X. Liu, and X. Ye, "Synergistic operation of electricity and natural gas networks via ADMM," *IEEE Trans. Smart Grid*, vol. 9, no. 5, pp. 4555-4565, Sept. 2018.
- [14] C. Wang, W. Wei, J. Wang, L. Bai, Y. Liang, and T. Bi, "Convex optimization based distributed optimal gas-power flow calculation," *IEEE Trans. Sustain. Energy*, vol. 9, no. 3, pp. 1145-1156, July 2018.
- [15] C. He, L. Wu, T. Liu, and M. Shahidehpour, "Robust co-optimization scheduling of electricity and natural gas systems via ADMM," *IEEE Trans. Sustain. Energy*, vol. 8, no. 2, pp. 658-670, April 2017.
- [16] Y. He *et al.*, "Decentralized optimization of multi-area electricity-natural gas flows based on cone reformulation," *IEEE Trans. Power Syst.*, vol. 33, no. 4, pp. 4531-4542, July 2018.
- [17] C. Borraz-Sánchez, R. Bent, S. Backhaus, H. Hijazi, and P. Hentenryck, "Convex relaxations for gas expansion planning," *INFORMS J. Comput.*, vol. 28, no. 4, pp. 645-656, 2016.
- [18] T. Lipp and S. Boyd, "Variations and extension of the convex-concave procedure," *Optim. Eng.*, vol. 17, pp. 263-287, 2016.
- [19] C. M. Correa-Posada and P. Sanchez-Martin, "Gas network optimization: A comparison of piecewise linear models," 2014 [Online]. Available: http://www.optimization-online.org/DB_HTML/2014/10/4580.html
- [20] R. Takapoui, N. Moehle, S. Boyd, Bemporad, and A. Bemporad, "A simple effective heuristic for embedded mixed-integer quadratic programming," in *Proc. Am. Control Conf.*, Boston, Massachusetts, 2016, pp. 5619-5625.
- [21] C. Chen, B. He, Y. Ye, and X. Yuan, "The direct extension of ADMM for multi-block convex minimization problems is not necessarily convergent," *Math. Program.*, vol. 155, no. 1, pp. 57-79, Jan. 2016.
- [22] W. Deng, M.-J. Lai, Z. Peng, and W. Yin, "Parallel multi-block ADMM with $o(1/k)$ convergence," *J. Sci. Comput.*, vol. 71, no. 2, pp. 712-736, May 2017.
- [23] J. Lavaei and S. H. Low, "Zero Duality Gap in Optimal Power Flow Problem," *IEEE Trans. Power Syst.*, vol. 27, no. 1, pp. 92-107, Feb. 2012.
- [24] S. Chen, A.J. Conejo, R. Sioshansi, and Z. Wei, "Unit commitment with an enhanced natural gas-flow model", *IEEE Trans. Power Syst.*, vol. 34, no. 5, pp. 3729 – 3738, 2019.
- [25] LMNO Engineering. Weymouth, Panhandle A and B equations for Compressible Gas Flow. [Online]. Available: <https://www.lmnoeng.com/Flow/weymouth.php>
- [26] D. Wolf and Y. Smeers, "The gas transmission problem solved by an extension of the simplex algorithm," *Manage. Sci.*, vol. 46, no. 11, pp. 1454-1465, Nov. 2000.
- [27] [Online]. Available: <https://sites.google.com/site/rongpengliu1991/>
- [28] A. Goncalves and X. Liu, "Two-block vs. multi-block ADMM: an empirical evaluation of convergence," [Online]. Available: <https://arxiv.org/pdf/1907.04524.pdf>